HHS Public Access

Author manuscript

Neuroimage. Author manuscript; available in PMC 2018 February 01.

Published in final edited form as:

Neuroimage. 2017 February 01; 146: 320–326. doi:10.1016/j.neuroimage.2016.11.054.

Cerebrovascular reactivity mapping without gas challenges

Peiying Liu[a,*], **Yang Li**[a,b], **Marco Pinho**[c], **Denise C. Park**[d], **Babu G. Welch**[c,e], and **Hanzhang Lu**[a]

[a]Department of Radiology, Johns Hopkins University School of Medicine, Baltimore, MD 21287

[b]Biomedical Engineering Graduate Program, UT Southwestern Medical Center, Dallas, TX 75390

[c]Department of Radiology, UT Southwestern Medical Center, Dallas, TX 75390

[d]Center for Vital Longevity, School of Behavioral and Brain Sciences, University of Texas at Dallas, Dallas, TX 75235

[e]Department of Neurological Surgery, UT Southwestern Medical Center, Dallas, TX 75390

Abstract

Cerebrovascular reactivity (CVR), the ability of cerebral vessels to dilate or constrict, has been shown to provide valuable information in the diagnosis and treatment evaluation of patients with various cerebrovascular conditions. CVR mapping is typically performed using hypercapnic gas inhalation as a vasoactive challenge while collecting BOLD images, but the inherent need of gas inhalation and the associated apparatus setup present a practical obstacle in applying it in routine clinical use. Therefore, we aimed to develop a new method to map CVR using resting-state BOLD data without the need of gas inhalation. This approach exploits the natural variation in respiration and measures its influence on BOLD MRI signal. In this work, we first identified a surrogate of the arterial CO_2 fluctuation during spontaneous breathing from the global BOLD signal. Second, we tested the feasibility and reproducibility of the proposed approach to use the above-mentioned surrogate as a regressor to estimate voxel-wise CVR. Third, we validated the "resting-state CVR map" with a conventional CVR map obtained with hypercapnic gas inhalation in healthy volunteers. Finally, we tested the utility of this new approach in detecting abnormal CVR in a group of patients with Moyamoya disease, and again validated the results using the conventional gas inhalation method. Our results showed that global BOLD signal fluctuation in the frequency range of 0.02–0.04 Hz contains the most prominent contribution from natural variation in arterial CO_2. The CVR map calculated using this signal as a regressor is reproducible across runs (ICC=0.91±0.06), and manifests a strong spatial correlation with results measured with a conventional hypercapnia-based method in healthy subjects ($r=0.88$, $p<0.001$). We also found that resting-state CVR was able to identify vasodilatory deficit in patients with steno-occlusive disease,

*Corresponding author. Peiying Liu, Ph.D. Department of Radiology Johns Hopkins University School of Medicine 600 N. Wolfe Street, Park 324 Baltimore, MD 21287 Tel.: 410 955 4173 Fax: 410 614 1977 peiying.liu@jhu.edu.

Conflicts of interest

The authors have no conflicts of interest or financial disclosures to report.

the spatial pattern of which matches that obtained using the conventional gas method (r=0.71±0.18). These results suggest that CVR obtained with resting-state BOLD may be a useful alternative in detecting vascular deficits in clinical applications when gas challenge is not feasible.

Keywords

Cerebrovascular reactivity; resting-state BOLD fMRI; global signal; spontaneous CO_2 fluctuation; hypercapnia (CO_2) inhalation; Moyamoya disease

1. Introduction

Cerebrovascular reactivity (CVR) is a measure of the dilatory function of cerebral blood vessels. Compared to other vascular measures such as cerebral blood flow (CBF) and cerebral blood volume (CBV), CVR is thought to be a more specific indicator of vascular health. CVR mapping has been shown to provide valuable information in the evaluation of various cerebrovascular conditions, including arterial stenosis (Donahue et al., 2013; Gupta et al., 2012; Mandell et al., 2008; Mikulis et al., 2005), stroke (Geranmayeh et al., 2015), small vessel disease (Greenberg, 2006), brain tumors (Zaca et al., 2014), traumatic brain injury (Chan et al., 2015; Kenney et al., 2016), substance abuse (Han et al., 2008), and normal aging (Gauthier et al., 2013; Lu et al., 2011). CVR also has important utility in normalizing blood-oxygenation level dependent (BOLD) fMRI signal to differentiate neuronal from vascular alternations in brain function (Liu et al., 2013a; Liu et al., 2013b).

At present, CVR mapping is typically performed using hypercapnic gas inhalation as a vasoactive challenge while collecting perfusion sensitive MRI images (Lu et al., 2014; Spano et al., 2013; Wise et al., 2007; Yezhuvath et al., 2009). Hypercapnic gas inhalation increases the blood concentration of CO_2, which, as a potent vasodilator, dilates blood vessels and increases cerebral perfusion (Brian, 1998). CVR can then be quantified by the BOLD signal changes associated with CO_2 inhalation. Although the BOLD signal is not a direct measure of CBF change in the brain and thus may be confounded by changes in cerebral oxygen metabolism (Xu et al., 2011), it is often preferred over perfusion signal (e.g. using arterial-spin-labeling MRI) due to its higher signal-to-noise ratio (SNR). This CVR mapping method has been successfully applied in a number of research studies in healthy and chronic disease patients (Donahue et al., 2013; Donahue et al., 2014; Han et al., 2008; Liu et al., 2013b; Lu et al., 2011; Mandell et al., 2008; Marshall et al., 2014; Mikulis et al., 2005; Thomas et al., 2013). However, the inherent need of gas inhalation and the associated apparatus setup requires additional time and expertise for handling and monitoring, which may limit the applications of this technique. This is especially the case when examining acute patients (e.g., acute stoke, acute traumatic brain injury). Breath-holding is another approach to manipulate blood CO_2 concentration (Kastrup et al., 1998; Murphy et al., 2011; Tancredi and Hoge, 2013; Zaca et al., 2014). But the requirement of subject's cooperation in performing breath-holding tasks also makes it difficult for patients with acute or severe conditions.

Therefore, in the present work, we aim to show the proof-of-principle of a new CVR mapping approach that does not require gas inhalation. This approach utilizes the natural

variation in respiration over time as an intrinsic vasoactive stimulus. A surrogate of fluctuations in arterial CO_2 can be extracted from global BOLD signal. Global, non-region-specific fluctuation in BOLD MRI signal is known to be attributed to several mechanisms, including cardiac cycle, breathing cycle, scanner thermal noise, slow physiological variations, and potentially whole-brain neural fluctuation (Birn et al., 2006; Chang et al., 2009; Glover et al., 2000; Wise et al., 2004; Wong et al., 2013). We hypothesize that the signal component association with respiratory variation can be extracted by advanced acquisition and analysis schemes of the global BOLD signal, which can then serve as a regressor for voxel-wise estimation of CVR, all from the resting-state BOLD data. We conducted four studies to test this hypothesis. Firstly, we identified the component in the global BOLD signal that has the best correspondence to end-tidal (Et) CO_2 time course at rest. Secondly, we tested the feasibility and reproducibility of performing voxel-wise calculation of CVR using the global BOLD as a regressor. Thirdly, we validated the "resting CVR map" with the conventional CVR map obtained by hypercapnic gas inhalation in healthy volunteers. Finally, we tested the utility of this new approach in detecting abnormal CVR in a group of patients with Moyamoya disease, a cerebrovascular disease characterized by intracranial arterial stenosis, and again validated the results using the conventional gas inhalation methods.

2. Materials and methods

2.1 General

All MR imaging experiments were conducted on 3 Tesla MR system (Philips Medical System, Best, The Netherlands). Foam padding was placed around the head to minimize motion. The study protocols were approved by the Institutional Review Boards of the Johns Hopkins University School of Medicine, the University of Texas Southwestern Medical Center and the University of Texas at Dallas. Written informed consent was obtained from all participants before the MRI scans.

Four studies were performed in separate participants. Study 1 and 4 were performed solely for the purpose of this report. Study 2 and 3 used resting-state BOLD data collected as part of our previous studies (Liu et al., 2013a; Tung et al., 2013). Data from a total of 48 participants are included.

2.2 Study 1: Identification of CO_2 related signal component from global BOLD

It is known that the origins of the global BOLD signal include many components. Therefore, the purpose of this study was to experimentally determine which frequency range of the global BOLD signal at rest contains the best correspondence to blood CO_2 concentration. Five healthy volunteers (age 35 ± 13 years, 3 males and 2 females) were scanned using a 32-channel receive-only head coil. The body coil was used for RF transmission. During the resting-state BOLD scan, the subject wore a nasal cannula (Salter Labs, Arvin, CA) through which the $EtCO_2$ was recorded using a capnograph device (Capnogard, Model 1265, Novametrix Medical Systems, CT). Imaging parameters of the BOLD scan were: single-shot gradient-echo EPI, Field-of-view (FOV) = 220×220×30 mm^3, voxel size=3.44×3.44×5mm^3, TR/TE=270/20ms, SENSE factor = 2, 6 axial slices with 1mm gap, 900 dynamics. The

imaging slices were positioned parallel to the anterior commissure -posterior commissure (AC-PC) line, with the last slice centered on the AC-PC line.

Data analysis was conducted using the software Statistical Parametric Mapping (SPM) (University College London, UK) and in-house MATLAB (MathWorks, Natick, MA) scripts. Pre-processing of the BOLD image series included motion correction, smoothing using a Gaussian filter with a full-width-half-maximum (FWHM) of 8 mm, and linear detrending. The $EtCO_2$ time course was shifted to account for the time it takes for the blood to travel from the lung to the heart and then to the brain, using a step-wise searching procedure described previously (Yezhuvath et al., 2009). The shifted $EtCO_2$ time course was in sync with the BOLD images, and was used for the following analysis.

To identify the best frequency component for the extraction of CO_2-related signal from the BOLD signal, the BOLD images were filtered into five different frequency bands: 0–0.01 Hz, 0.01–0.02 Hz, 0.02–0.04 Hz, 0.04–0.08 Hz, 0.08–0.2 Hz, and the global BOLD time course for each frequency band was obtained. The frequency width was set to be larger at higher frequencies because signal power decays at higher frequencies. Signal frequencies above 0.2 Hz were not tested because those signal components are expected to be primarily due to cardiac and breathing cycles and there is minimal $EtCO_2$ signal in that frequency range (Birn et al., 2006; Chang et al., 2009; Wise et al., 2004). The BOLD signal time course was then spatially averaged to minimize scanner thermal noise, generating a reference BOLD time course for each frequency range. The cross-correlation coefficient (r) between the reference BOLD time course and $EtCO_2$ time course was calculated for each frequency band. Paired t-tests were performed to compare the r values across the frequency bands to identify the band that provides the highest R, which was used as the optimal frequency range for CVR calculations in the following studies.

An exploratory analysis was also performed to compare the statistical significance (indicated by Z score) of voxel-wise regression using the filtered reference BOLD signal as regressor to that using $EtCO_2$ time course as regressor following a previous study (Golestani et al., 2016). Z scores from all brain voxels were considered. Paired t-tests were performed to evaluate the significance of the comparison between the two methods. The p value <0.05 is considered significant.

2.3 Study 2: Feasibility and reproducibility

Study 2 examined the feasibility of using resting-state BOLD fMRI to map CVR, and evaluated the reproducibility of this approach. This study was done by using resting state data collected in our previous study (Tung et al., 2013). Ten healthy subjects (age 28±7 years, 6 males and 4 females) underwent a 35-minute session consisting of 7 resting state BOLD scans of 5 minutes each. An 8-channel receive-only head coil was used. The BOLD imaging parameters were: single-shot gradient-echo EPI, TR/TE=1000/25ms, FOV= 220×220×104 mm^3, voxel size 3.4×3.4×4mm^3, 21 axial slices with 1mm gap covering the whole cerebrum, 300 dynamics. Compared to Study 1, the data in this study provided a substantially larger spatial coverage, although the temporal resolution was lower.

The data analysis followed the chart shown in Figure 1. The pre-processing was identical to that used in Study 1. The temporal filtering of the BOLD time course used the optimal frequency band determined from Study 1. A whole-brain mask obtained from a T_1-weighted MPRAGE image was used as a reference mask and the voxels inside the mask were averaged to yield the reference time course. A linear regression analysis was then performed in which the reference time course was the independent variable and individual voxel's time course was the dependent variable, yielding a CVR index for each voxel. By normalizing the CVR index to a mean value calculated from the reference mask, a resting-state CVR map was obtained. We note that the resting-state CVR map is in relative units. To evaluate the reproducibility of the resting state CVR maps, intraclass correlation (ICC) analysis was performed across multiple runs of the data (Shrout and Fleiss, 1979). For this study, two-way model, average-measures ICC values were calculated.

2.4 Study 3: Validation of resting-state CVR with gas-inhalation based method

Twenty-six healthy subjects (age 28 ± 5 years, 12 males and 14 females) underwent a 5 min resting-state BOLD scan and a 7 min hypercapnia BOLD scan (Liu et al., 2013a). An 8-channel receive-only head coil was used. The imaging parameters were identical between the two scans: TR/TE=2000/25ms, FOV=220×220×150.5mm^3, voxel size 3.4×3.4×3.5mm^3, 43 axial slices without gap. During the hypercapnia scan, subjects breathed room-air and 5% CO_2 (mixed with 21% O2 and 74% N2) in an interleaved fashion (switching every 1 min) while BOLD EPI images were acquired continuously. $EtCO_2$ was recorded throughout the breathing task.

A regression analysis between $EtCO_2$ and the MRI time course yielded the gas-inhalation-based CVR map (Lu et al., 2014; Yezhuvath et al., 2009). The resting-state CVR map (in relative units) was obtained following the procedures developed in Study 2 (Figure 1). Spatial correlation between the resting-state and gas-inhalation CVR maps was calculated as the Pearson product-moment coefficient. For easy comparison, the gas-inhalation CVR map was also normalized to its whole-brain value.

2.5 Study 4: Evaluation of Moyamoya patients

Seven patients with Moyamoya Disease (age 39 ± 10 years, 1 male and 6 females) were recruited. Moyamoya Disease is a steno-occlusive cerebrovascular disease characterized by severe narrowing/blockage of the anterior and middle cerebral vessels. The specific diagnosis of each patient in this study is listed in Table 1. Four patients had unilateral stenosis and three had bilateral stenosis. Each patient underwent a 9 min resting-state BOLD scan and a gas inhalation scan of 9 min. The imaging parameters for both the breathing task and the resting-state scan were: BOLD sequence, FOV = 205×205×151 mm^3, TR/TE=1510/21ms, 3.2mm isotropic voxels, whole brain coverage using 36 slices with 1mm gap. The gas inhalation scan utilized the concomitant CO_2/O_2 modulation paradigm so that CVR and venous CBV maps were obtained simultaneously. Details of the concomitant CO_2/O_2 modulation and data analysis were described previously (Liu et al., 2016). An ASL scan was performed to obtain CBF. The imaging parameters of the ASL scan were: 2D multi-slice acquisition, labeling duration=1650ms, post-labeling delay = 1525ms, TR/TE=4260/14 ms, FOV=240×240×145.5mm^3, voxel size 3×3×5mm^3, whole-brain coverage

using 29 axial slices without gap. Anatomical images of FLAIR, T_1-weighted MPRAGE, and time-of-flight (TOF) angiogram were also obtained. All patients were scanned with a 32-channel receive-only head coil. The body coil was used for RF transmission.

Resting-state and gas-inhalation CVR maps were obtained using procedures described above. Both maps are in relative units. In these analyses, we used cerebellum gray matter as the reference region because posterior circulation is usually preserved (as verified by the TOF angiogram) in Moyamoya patients. Deficit regions as identified by resting-state and gas-inhalation CVR were compared. Quantitative comparison between the two methods was performed using scatter plot and spatial correlation. CBF maps were obtained following the ASL white paper (Alsop et al., 2015).

3. Results

3.1 Study 1

Figure 2 shows cross-correlation coefficients between $EtCO_2$ and BOLD signal time courses for different frequency ranges. It can be seen that the correlation is highest when the time courses are filtered at the 0.02–0.04 Hz frequency range. Paired t-tests showed that the correlation at 0.02–0.04 Hz is significantly higher than all other frequency bands except for 0.01–0.02 Hz (Figure 2). Indeed, the peak correlation appeared at the 0.02–0.04 Hz for every participant in the study. These observations suggested that BOLD signal at the frequency range of 0.02–0.04 Hz provides the best estimation of the spontaneous fluctuation of blood CO_2 concentration, relative to other frequency bands. Therefore, in the following studies, the BOLD time series were all filtered to 0.02–0.04 Hz for the calculation of CVR map using resting-state data.

Comparing the methods using global BOLD signal (filtered to 0.02–0.04 Hz) and $EtCO_2$ time course, the statistical significance of voxel-wise regression is considerably greater when using the global BOLD signal ($p=0.001$). The resulting voxel-wise Z scores were 17.9±3.2 and 4.0±2.7 for global BOLD and $EtCO_2$ methods, respectively. Similarly, we found that 90±5% of voxels in the brain has a statistically significance Z score ($Z>3$) using the global BOLD signal as a regressor, as compared to 50±20% using $EtCO_2$ as the regressor ($p=0.014$).

3.2 Study 2

Figure 3 demonstrates the resting-state CVR maps obtained from seven consecutive scans from a representative subject. The maps showed clear gray matter – white matter contrast, which is consistent across different scans. The resting-state CVR maps of all scans from all subjects are shown in Supplementary Figure S1. The ICC values were found to be 0.91±0.06 (mean±standard deviation) across 10 subjects (range from 0.79 to 0.98), indicating a good reproducibility of the resting-state CVR maps.

3.3 Study 3

Figure 4a displays group-averaged CVR maps obtained from the resting-state and hypercapnia scans. Visual inspection suggests that the two CVR maps, although obtained by

different techniques, have virtually identical image contrast. The gray matter has larger CVR than white matter, and voxels containing veins shows the highest CVR values due to the blood volume effect. The voxels containing veins were identified by visual inspection based on knowledge of the vessel anatomy of large draining veins. Consistency of the two CVR maps was confirmed by quantitative analysis of their scatter plot, shown in Figure 4b. There was a strong spatial correlation (r=0.88) between the two maps. The individual resting-state and hypercapnia-derived CVR maps of all subjects are shown in Supplementary Figure S2. To compare the sensitivity of the resting-state CVR method with the standard gas method, Figure 4c shows the histogram of Z-statistics of the resting-state and hypercapnia-based techniques. It can be seen that the resting-state method (Z=7.47±1.75, N=26) is less sensitive compared to the hypercapnia CVR mapping technique (Z=11.94±2.54, N=26), as expected.

3.4 Study 4

The demographic information of the Moyamoya patients is shown in Table 1. Figure 5 shows CVR maps from resting-state and hypercapnia scans of all seven patients. For reference, the patients' MRI angiograms are also shown, illustrating the specific stenosis site of each patient (red arrows). T_1-MPRAGE, FLAIR, CBF and venous CBV images are also displayed. Reduced CVR was observed in the disease territories in all patients. Resting-state CVR maps were found to reveal a similar deficit pattern as the hypercapnia CVR maps, suggesting that CVR measured with resting-state BOLD fMRI can provide similar information of cerebrovascular dysfunction as that obtained using a conventional hypercapnia-based method. Scatter plots between the two CVR maps are shown in Figure 5 (bottom row). Their spatial correlation coefficient was 0.71±0.18. We have also investigated resting-state CVR mapping using the frequency bands other than 0.02–0.04 Hz, and found that the resulted resting-state CVR maps were less consistent with the hypercapnia CVR map (Supplementary Figure S3).

Comparing to CBF and venous CBV maps, the two CVR maps showed their unique deficit pattern, suggesting that the resting-state CVR we obtained measures the specific vascular function as the hypercapnia CVR.

4. Discussion

In this report, we propose a new method to map cerebrovascular reactivity without the need of gas inhalation. We identified that global BOLD signal fluctuation in the frequency range of 0.02–0.04 Hz contains the most prominent contribution from natural variation in arterial CO_2. We then utilized this signal as a regressor for CVR estimation from the resting-state BOLD fMRI data. Our results showed that the CVR map calculated with this method is reproducible across runs, and manifests a strong spatial correlation with results measured with a conventional hypercapnia-based method. Resting-state CVR was able to identify vasodilatory deficits in patients with steno-occlusive disease, the spatial pattern of which is similar to that using conventional gas method.

CVR indicates the ability of blood vessels to dilate upon demand, and is thought to be a specific marker of vascular health compared to cerebral perfusion, which may be affected by non-vascular factors such as neural activity, metabolism, and consumption of caffeine (Chen

and Parrish, 2009; Fujishima et al., 1971). CVR has shown an important value in research studies involving chronic ischemic conditions such as atherosclerotic arterial steno-occlusive disease and Moyamoya disease (Donahue et al., 2013; Gupta et al., 2012; Mandell et al., 2008; Mikulis et al., 2005; Pandya et al., 2015). However, despite its potential, CVR mapping has not been used in large-scale clinical trials or routine clinical practice. One of the most important limitations of this method is that CVR mapping using gas-inhalation is typically viewed as cumbersome (although recent development in breathing apparatus (Lu et al., 2014; Tancredi et al., 2014) has begun to address these issues) and thus cannot be applied routinely. There are additional concerns of using gas challenges in acute or severely ill patients, as they may not tolerate or report their intolerance of hypercapnia. It has also been suggested that patients with significant pulmonary or cardiac disease should not be given gas challenge (Moreton et al., 2016). Therefore, there is significant clinical value to develop a CVR mapping method that does not require gas inhalation. The present work is one of such efforts to measure CVR using resting-state BOLD data. We have shown that resting-state CVR maps have a strong correlation with conventional, gas-inhalation based CVR maps, although its overall sensitivity, as measured by Z-statistic, is lower. We also note that the resting-state CVR mapping is based on the spontaneous fluctuation of blood CO_2 content, which is in the range of 2–4 mmHg. This natural variation is much smaller than the change induced by 5% CO_2 breathing (usually 8–10 mmHg), but is more relevant to the degree of daily neural activation induced blood flow changes. Given the non-linear relationship between blood CO2 content and CBF change (Fox et al., 1992; Ito et al., 2003), it is expected that the BOLD signal may also change non-linearly with blood CO2.

Resting-state fMRI data are known to contain information about the brain's vasculature, in addition to its common use of mapping functional connectivity (Birn et al., 2006; Wise et al., 2004). Kannurpatti and Biswal showed that the resting-state fluctuation amplitude (RSFA), computed as the temporal standard deviation of the BOLD time series, is correlated with CVR measured with breath-holding (Kannurpatti and Biswal, 2008). Jahanian et al. further showed that coefficient of variance (CV, standard deviation divided by mean) of the BOLD signal was significantly higher in hypertensive elderly subjects with chronic kidney disease than in young healthy volunteers (Jahanian et al., 2014). Other studies have explored a parameter that quantifying the degree of low-frequency variation of the BOLD signal, referred to as Amplitude of low-frequency fluctuations (ALFF), and have demonstrated a correlation between ALFF and hypercapnia-derived CVR (Di et al., 2013; Kazan et al., 2016). These methods have not attempted to differentiate various components of the BOLD signal, thus may contain a variety of physiological origins. In our study, we considered the multi-factorial mechanism of the global BOLD signal and developed specific acquisition and analysis schemes to maximally isolate signal component associated with natural fluctuation in blood CO_2. The effects of cardiac and respiratory cycles on the BOLD time course were alleviated by acquiring data at a relatively high temporal frequency, thus such effects can be removed by low-pass filtering. Scanner thermal noise was minimized by spatially averaging a large number of voxels, e.g. the whole-brain, and by using the averaged signal as a regressor in CVR calculation. Further effort to obtain the signal component that is most relevant to CO_2 fluctuation was undertaken by identifying the frequency band (0.02–0.04 Hz) that shows the higher correlation with end-tidal CO_2. A few studies have also been

reported to use resting-state fMRI data to estimate blood transit time in the brain (Amemiya et al., 2014; Christen et al., 2015; Tong and Frederick, 2014). We have tried to obtain the voxel-wise delay following a previous study (Christen et al., 2015) and apply it in resting-state CVR mapping. However, the resulted CVR maps were noisy, probably due to the low SNR in resting-state delay mapping. Therefore, we did not account for voxel-wise blood transit delay in our CVR analyses. As a result, the deficit regions in the CVR maps of the Moyamoya patients (Figure 5) reflect both diminished CVR and lengthened blood transit delay in those regions.

Recently, two studies reported the use of $EtCO_2$ time course recorded during the resting-state BOLD scan as a regressor to map CVR in healthy volunteers (Golestani et al., 2016; Lipp et al., 2015). Compared to these previous studies, the present study is the first to apply these methodologies in patients with cerebrovascular diseases. Moreover, the present work has primarily focused on the use of filtered global BOLD signal as a regressor, rather than $EtCO_2$ as the regressor, due to the following reasons. First, when comparing the $EtCO_2$ and global BOLD methods, we found that the global BOLD method provided significantly better CVR maps (in terms of Z-scores). This is because $EtCO_2$ has a lower sampling frequency, e.g. one measure every 4 seconds, whereas the resulting BOLD signal change has a higher sampling frequency, e.g. one measure every 270 ms. Thus, a regression analysis between these two time series requires substantial temporal interpolation. One could downsample the BOLD images to match the sampling rate of EtCO2 and conduct the regression analysis. However, that means a large fraction of the BOLD data is discarded. Additionally, CO_2 concentration time course in the lung will be slightly different from that in the brain due to dispersion. This could further reduce the degree of association between $EtCO_2$ and BOLD signal time courses. Moreover, the placement of $EtCO_2$ recording apparatus may take some additional setup time and wearing the apparatus for an extended period of time (i.e. having the tips of the nasal cannula at the nostril for the entire session, not just during the resting CVR scan) may cause some discomfort. For most cerebrovascular diseases which are usually regional, a relative map measured by resting-state CVR is sufficient to delineate deficit brain areas. If an absolute CVR (e.g. in %/mmHg) is desired, $EtCO_2$ recording using nasal cannula (as done in our Study 1) can be added to the procedure. However, to obtain the highest statistical significance, we still recommend the use of filtered global BOLD as the regressor. The $EtCO_2$ recording is thus mainly used for the conversion from relative units to mmHg units.

This study has a few limitations. First, the resting-state CVR maps we obtained are in relative units, instead of in absolute unit of %/mmHg CO_2. As mentioned earlier, recording of $EtCO_2$ can be added if absolute values are desired. Second, we have empirically found that the global BOLD signal within the frequency range of 0.02–0.04 Hz has the strongest correlation with $EtCO_2$. However, it is plausible that the signal in this frequency range still contains some contributions from non-CO_2 related sources, for example, global fluctuations in neural activity due to vigilance changes (Liu, 2013; Wong et al., 2013), subject motion and heart rate changes. We are conducting further studies with simultaneous fMRI/EEG to investigate the extent of this contribution. Third, for Study 1, we did not have hypercapnia CVR map to calculate the spatial correlation between resting-state and hypercapnia CVR maps.

5. Conclusions

In this work, we developed a new method to map cerebrovascular reactivity using resting-state BOLD data without the need of gas inhalation or breath-holding. Our results have shown that resting-state CVR maps obtained by this method are reproducible, and are highly consistent with conventional, CO_2-inhalation-based CVR maps. This method may be a useful alternative in detecting vascular deficits in clinical applications when gas challenge is not feasible.

Supplementary Material

Refer to Web version on PubMed Central for supplementary material.

Acknowledgments

This study was supported in part by NIH R01 AG042753 (to H.L.), NIH R01 MH084021 (to H.L.), NIH R01 NS067015 (to H.L.), NIH R01 AG047972 (to H.L.), NIH R21 NS095342 (to H.L.), NIH R21 NS085634 (to P.L.), NIH R37 AG006265 (to D.C.P.) and NIH P41 EB015909 (to H.L.).

Reference

Alsop DC, Detre JA, Golay X, Gunther M, Hendrikse J, Hernandez-Garcia L, Lu H, MacIntosh BJ, Parkes LM, Smits M, van Osch MJ, Wang DJ, Wong EC, Zaharchuk G. Recommended implementation of arterial spin-labeled perfusion MRI for clinical applications: A consensus of the ISMRM perfusion study group and the European consortium for ASL in dementia. Magn Reson Med. 2015; 73:102–116. [PubMed: 24715426]

Amemiya S, Kunimatsu A, Saito N, Ohtomo K. Cerebral hemodynamic impairment: assessment with resting-state functional MR imaging. Radiology. 2014; 270:548–555. [PubMed: 24072777]

Birn RM, Diamond JB, Smith MA, Bandettini PA. Separating respiratory-variation-related fluctuations from neuronal-activity-related fluctuations in fMRI. Neuroimage. 2006; 31:1536–1548. [PubMed: 16632379]

Brian JE Jr. Carbon dioxide and the cerebral circulation. Anesthesiology. 1998; 88:1365–1386. [PubMed: 9605698]

Chan ST, Evans KC, Rosen BR, Song TY, Kwong KK. A case study of magnetic resonance imaging of cerebrovascular reactivity: a powerful imaging marker for mild traumatic brain injury. Brain Inj. 2015; 29:403–407. [PubMed: 25384127]

Chang C, Cunningham JP, Glover GH. Influence of heart rate on the BOLD signal: the cardiac response function. Neuroimage. 2009; 44:857–869. [PubMed: 18951982]

Chen Y, Parrish TB. Caffeine's effects on cerebrovascular reactivity and coupling between cerebral blood flow and oxygen metabolism. Neuroimage. 2009; 44:647–652. [PubMed: 19000770]

Christen T, Jahanian H, Ni WW, Qiu D, Moseley ME, Zaharchuk G. Noncontrast mapping of arterial delay and functional connectivity using resting-state functional MRI: a study in Moyamoya patients. J Magn Reson Imaging. 2015; 41:424–430. [PubMed: 24419985]

Di X, Kannurpatti SS, Rypma B, Biswal BB. Calibrating BOLD fMRI activations with neurovascular and anatomical constraints. Cereb Cortex. 2013; 23:255–263. [PubMed: 22345358]

Donahue MJ, Ayad M, Moore R, van Osch M, Singer R, Clemmons P, Strother M. Relationships between hypercarbic reactivity, cerebral blood flow, and arterial circulation times in patients with moyamoya disease. J Magn Reson Imaging. 2013 In-press.

Donahue MJ, Dethrage LM, Faraco CC, Jordan LC, Clemmons P, Singer R, Mocco J, Shyr Y, Desai A, O'Duffy A, Riebau D, Hermann L, Connors J, Kirshner H, Strother MK. Routine Clinical Evaluation of Cerebrovascular Reserve Capacity Using Carbogen in Patients With Intracranial Stenosis. Stroke. 2014; 45:2335–2341. [PubMed: 24938845]

Fox J, Gelb AW, Enns J, Murkin JM, Farrar JK, Manninen PH. The responsiveness of cerebral blood flow to changes in arterial carbon dioxide is maintained during propofol-nitrous oxide anesthesia in humans. Anesthesiology. 1992; 77:453–456. [PubMed: 1519782]

Fujishima M, Scheinberg P, Busto R, Reinmuth OM. The relation between cerebral oxygen consumption and cerebral vascular reactivity to carbon dioxide. Stroke. 1971; 2:251–257. [PubMed: 5111573]

Gauthier CJ, Madjar C, Desjardins-Crepeau L, Bellec P, Bherer L, Hoge RD. Age dependence of hemodynamic response characteristics in human functional magnetic resonance imaging. Neurobiol Aging. 2013; 34:1469–1485. [PubMed: 23218565]

Geranmayeh F, Wise RJ, Leech R, Murphy K. Measuring vascular reactivity with breath-holds after stroke: a method to aid interpretation of group-level BOLD signal changes in longitudinal fMRI studies. Hum Brain Mapp. 2015; 36:1755–1771. [PubMed: 25727648]

Glover GH, Li TQ, Ress D. Image-based method for retrospective correction of physiological motion effects in fMRI: RETROICOR. Magn Reson Med. 2000; 44:162–167. [PubMed: 10893535]

Golestani AM, Wei LL, Chen JJ. Quantitative mapping of cerebrovascular reactivity using resting-state BOLD fMRI: Validation in healthy adults. Neuroimage. 2016; 138:147–163. [PubMed: 27177763]

Greenberg SM. Small vessels, big problems. N Engl J Med. 2006; 354:1451–1453. [PubMed: 16598043]

Gupta A, Chazen JL, Hartman M, Delgado D, Anumula N, Shao H, Mazumdar M, Segal AZ, Kamel H, Leifer D, Sanelli PC. Cerebrovascular reserve and stroke risk in patients with carotid stenosis or occlusion: a systematic review and meta-analysis. Stroke. 2012; 43:2884–2891. [PubMed: 23091119]

Han JS, Mandell DM, Poublanc J, Mardimae A, Slessarev M, Jaigobin C, Fisher JA, Mikulis DJ. BOLD-MRI cerebrovascular reactivity findings in cocaine-induced cerebral vasculitis. Nat Clin Pract Neurol. 2008; 4:628–632. [PubMed: 18839005]

Ito H, Kanno I, Ibaraki M, Hatazawa J, Miura S. Changes in human cerebral blood flow and cerebral blood volume during hypercapnia and hypocapnia measured by positron emission tomography. J Cereb Blood Flow Metab. 2003; 23:665–670. [PubMed: 12796714]

Jahanian H, Ni WW, Christen T, Moseley ME, Kurella Tamura M, Zaharchuk G. Spontaneous BOLD signal fluctuations in young healthy subjects and elderly patients with chronic kidney disease. PLoS One. 2014; 9:e92539. [PubMed: 24651703]

Kannurpatti SS, Biswal BB. Detection and scaling of task-induced fMRI-BOLD response using resting state fluctuations. Neuroimage. 2008; 40:1567–1574. [PubMed: 18343159]

Kastrup A, Li TQ, Takahashi A, Glover GH, Moseley ME. Functional magnetic resonance imaging of regional cerebral blood oxygenation changes during breath holding. Stroke. 1998; 29:2641–2645. [PubMed: 9836778]

Kazan SM, Mohammadi S, Callaghan MF, Flandin G, Huber L, Leech R, Kennerley A, Windischberger C, Weiskopf N. Vascular autorescaling of fMRI (VasA fMRI) improves sensitivity of population studies: A pilot study. Neuroimage. 2016; 124:794–805. [PubMed: 26416648]

Kenney K, Amyot F, Haber M, Pronger A, Bogoslovsky T, Moore C, Diaz-Arrastia R. Cerebral Vascular Injury in Traumatic Brain Injury. Exp Neurol. 2016; 275(Pt 3):353–366. [PubMed: 26048614]

Lipp I, Murphy K, Caseras X, Wise RG. Agreement and repeatability of vascular reactivity estimates based on a breath-hold task and a resting state scan. Neuroimage. 2015; 113:387–396. [PubMed: 25795342]

Liu P, Hebrank AC, Rodrigue KM, Kennedy KM, Park DC, Lu H. A comparison of physiologic modulators of fMRI signals. Hum Brain Mapp. 2013a; 34:2078–2088. [PubMed: 22461234]

Liu P, Hebrank AC, Rodrigue KM, Kennedy KM, Section J, Park DC, Lu H. Age-related differences in memory-encoding fMRI responses after accounting for decline in vascular reactivity. Neuroimage. 2013b; 78:415–425. [PubMed: 23624491]

Liu P, Welch BG, Li Y, Gu H, King D, Yang Y, Pinho M, Lu H. Multiparametric imaging of brain hemodynamics and function using gas-inhalation MRI. NeuroImage. 2016

Liu TT. Neurovascular factors in resting-state functional MRI. Neuroimage. 2013; 80:339–348. [PubMed: 23644003]

Lu H, Liu P, Yezhuvath U, Cheng Y, Marshall O, Ge Y. MRI mapping of cerebrovascular reactivity via gas inhalation challenges. J Vis Exp. 2014

Lu H, Xu F, Rodrigue KM, Kennedy KM, Cheng Y, Flicker B, Hebrank AC, Uh J, Park DC. Alterations in cerebral metabolic rate and blood supply across the adult lifespan. Cereb Cortex. 2011; 21:1426–1434. [PubMed: 21051551]

Mandell DM, Han JS, Poublanc J, Crawley AP, Stainsby JA, Fisher JA, Mikulis DJ. Mapping cerebrovascular reactivity using blood oxygen level-dependent MRI in Patients with arterial steno-occlusive disease: comparison with arterial spin labeling MRI. Stroke. 2008; 39:2021–2028. [PubMed: 18451352]

Marshall O, Lu H, Brisset JC, Xu F, Liu P, Herbert J, Grossman RI, Ge Y. Impaired cerebrovascular reactivity in multiple sclerosis. JAMA Neurol. 2014; 71:1275–1281. [PubMed: 25133874]

Mikulis DJ, Krolczyk G, Desal H, Logan W, Deveber G, Dirks P, Tymianski M, Crawley A, Vesely A, Kassner A, Preiss D, Somogyi R, Fisher JA. Preoperative and postoperative mapping of cerebrovascular reactivity in moyamoya disease by using blood oxygen level-dependent magnetic resonance imaging. J Neurosurg. 2005; 103:347–355. [PubMed: 16175867]

Moreton FC, Dani KA, Goutcher C, O'Hare K, Muir KW. Respiratory challenge MRI: Practical aspects. NeuroImage: Clinical. 2016; 11:667–677. [PubMed: 27330967]

Murphy K, Harris AD, Wise RG. Robustly measuring vascular reactivity differences with breath-hold: normalising stimulus-evoked and resting state BOLD fMRI data. Neuroimage. 2011; 54:369–379. [PubMed: 20682354]

Pandya A, Gupta A, Kamel H, Navi BB, Sanelli PC, Schackman BR. Carotid artery stenosis: cost-effectiveness of assessment of cerebrovascular reserve to guide treatment of asymptomatic patients. Radiology. 2015; 274:455–463. [PubMed: 25225841]

Shrout PE, Fleiss JL. Intraclass correlations: uses in assessing rater reliability. Psychol Bull. 1979; 86:420–428. [PubMed: 18839484]

Spano VR, Mandell DM, Poublanc J, Sam K, Battisti-Charbonney A, Pucci O, Han JS, Crawley AP, Fisher JA, Mikulis DJ. CO2 blood oxygen level-dependent MR mapping of cerebrovascular reserve in a clinical population: safety, tolerability, and technical feasibility. Radiology. 2013; 266:592–598. [PubMed: 23204541]

Tancredi FB, Hoge RD. Comparison of cerebral vascular reactivity measures obtained using breath-holding and CO2 inhalation. J Cereb Blood Flow Metab. 2013; 33:1066–1074. [PubMed: 23571282]

Tancredi FB, Lajoie I, Hoge RD. A simple breathing circuit allowing precise control of inspiratory gases for experimental respiratory manipulations. BMC Res Notes. 2014; 7:235. [PubMed: 24725848]

Thomas BP, Yezhuvath US, Tseng BY, Liu PY, Levine BD, Zhang R, Lu HZ. Life-Long Aerobic Exercise Preserved Baseline Cerebral Blood Flow but Reduced Vascular Reactivity to CO2. Journal of Magnetic Resonance Imaging. 2013; 38:1177–1183. [PubMed: 23526811]

Tong Y, Frederick B. Tracking cerebral blood flow in BOLD fMRI using recursively generated regressors. Hum Brain Mapp. 2014; 35:5471–5485. [PubMed: 24954380]

Tung KC, Uh J, Mao D, Xu F, Xiao G, Lu H. Alterations in resting functional connectivity due to recent motor task. Neuroimage. 2013; 78:316–324. [PubMed: 23583747]

Wise RG, Ide K, Poulin MJ, Tracey I. Resting fluctuations in arterial carbon dioxide induce significant low frequency variations in BOLD signal. Neuroimage. 2004; 21:1652–1664. [PubMed: 15050588]

Wise RG, Pattinson KT, Bulte DP, Chiarelli PA, Mayhew SD, Balanos GM, O'Connor DF, Pragnell TR, Robbins PA, Tracey I, Jezzard P. Dynamic forcing of end-tidal carbon dioxide and oxygen applied to functional magnetic resonance imaging. J Cereb Blood Flow Metab. 2007; 27:1521–1532. [PubMed: 17406659]

Wong CW, Olafsson V, Tal O, Liu TT. The amplitude of the resting-state fMRI global signal is related to EEG vigilance measures. Neuroimage. 2013; 83:983–990. [PubMed: 23899724]

Xu F, Uh J, Brier MR, Hart J Jr, Yezhuvath US, Gu H, Yang Y, Lu H. The influence of carbon dioxide on brain activity and metabolism in conscious humans. J Cereb Blood Flow Metab. 2011; 31:58–67. [PubMed: 20842164]

Yezhuvath US, Lewis-Amezcua K, Varghese R, Xiao G, Lu H. On the assessment of cerebrovascular reactivity using hypercapnia BOLD MRI. NMR Biomed. 2009; 22:779–786. [PubMed: 19388006]

Zaca D, Jovicich J, Nadar SR, Voyvodic JT, Pillai JJ. Cerebrovascular reactivity mapping in patients with low grade gliomas undergoing presurgical sensorimotor mapping with BOLD fMRI. J Magn Reson Imaging. 2014; 40:383–390. [PubMed: 24338845]

Highlights

- A new method was proposed to map CVR without gas inhalation or breath-holding
- This method exploits natural variations in respiration and their effect on BOLD signal
- The resulted CVR maps were reproducible and consistent with CO_2-inhalation CVR maps
- This method can identify CVR deficit in patients with steno-occlusive disease
- This method may be a useful alternative to map CVR when gas challenges is not feasible

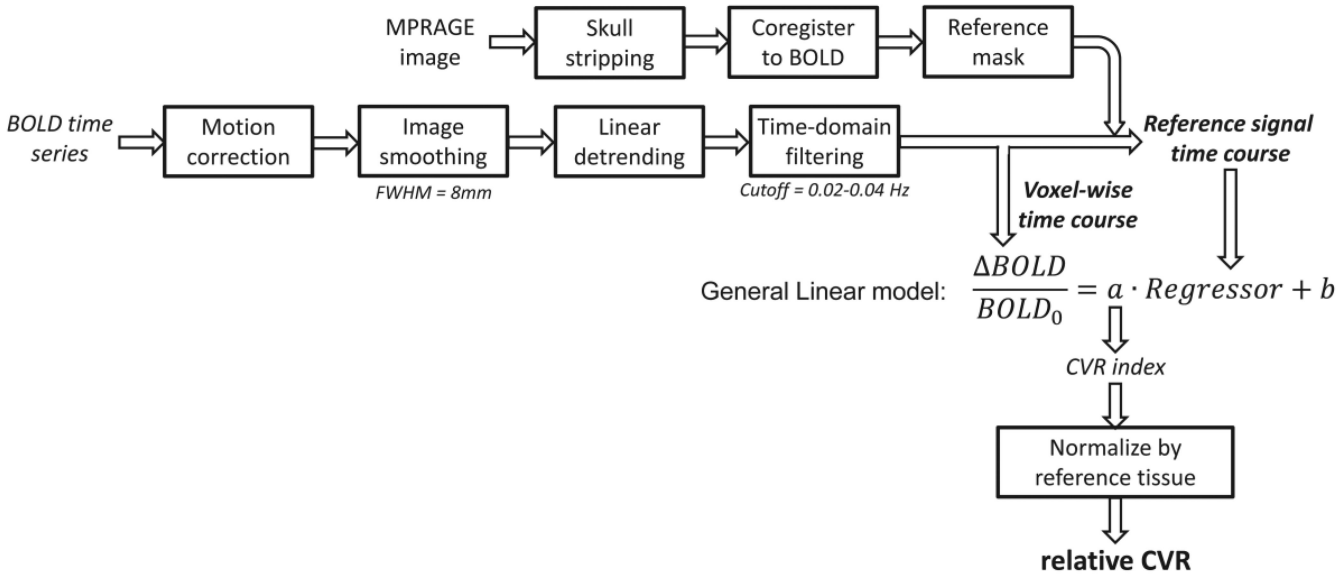

Figure 1.
Illustration of the data analysis scheme.

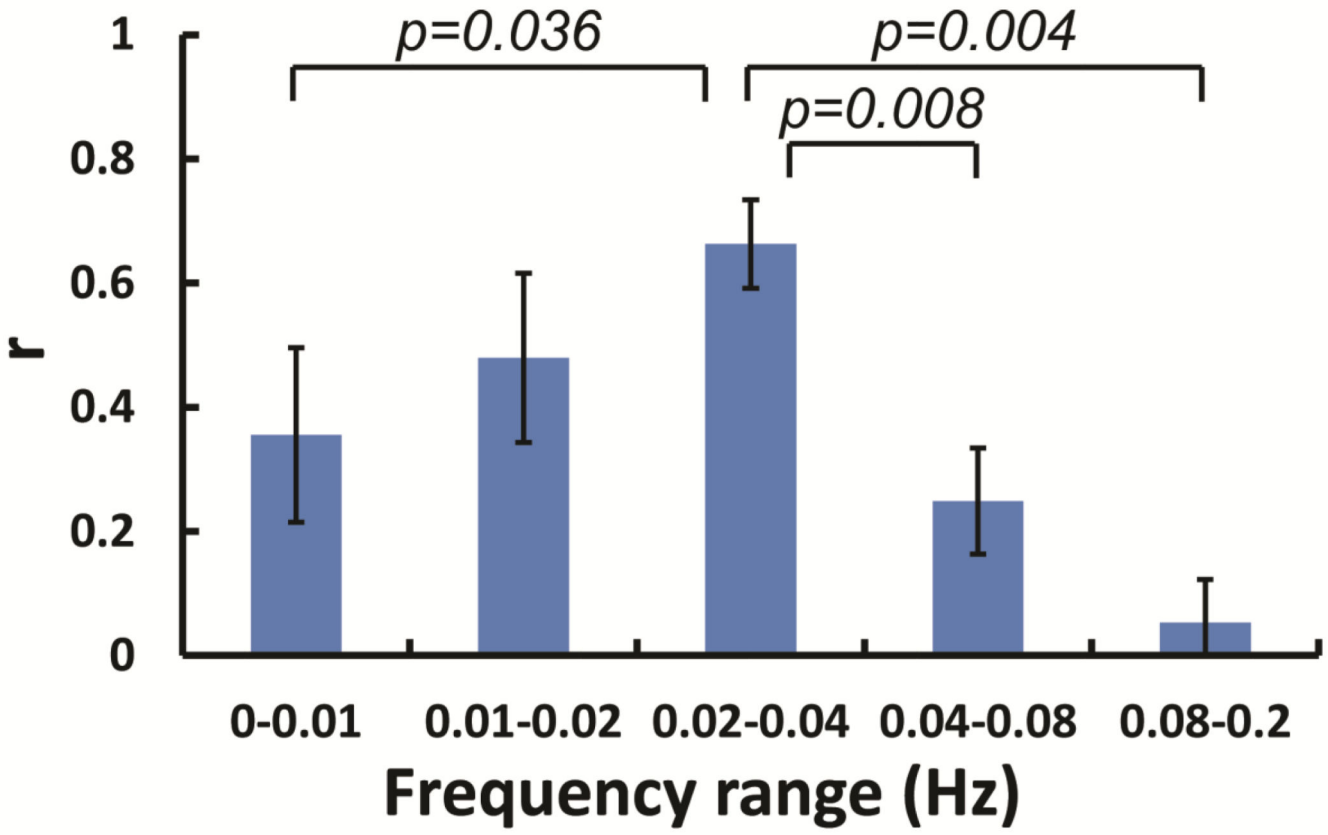

Figure 2.
The correlation between global BOLD signal and $EtCO_2$ time course at different frequency ranges (N=5). Error bars indicate standard error. The p-values are uncorrected.

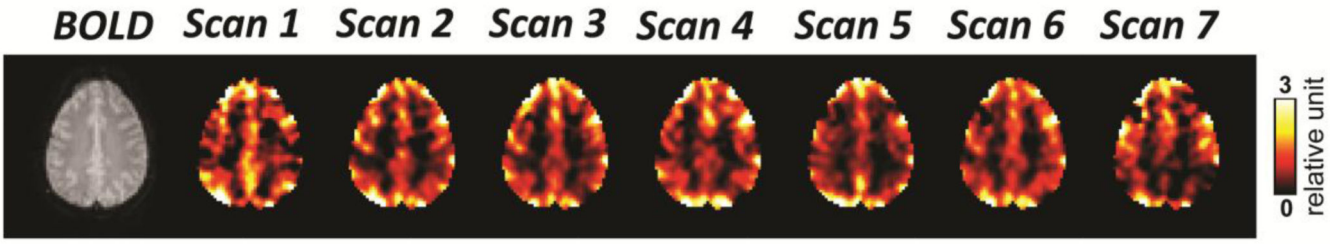

Figure 3.
CVR maps of seven consecutive resting-state BOLD fMRI scans from a representative healthy subject.

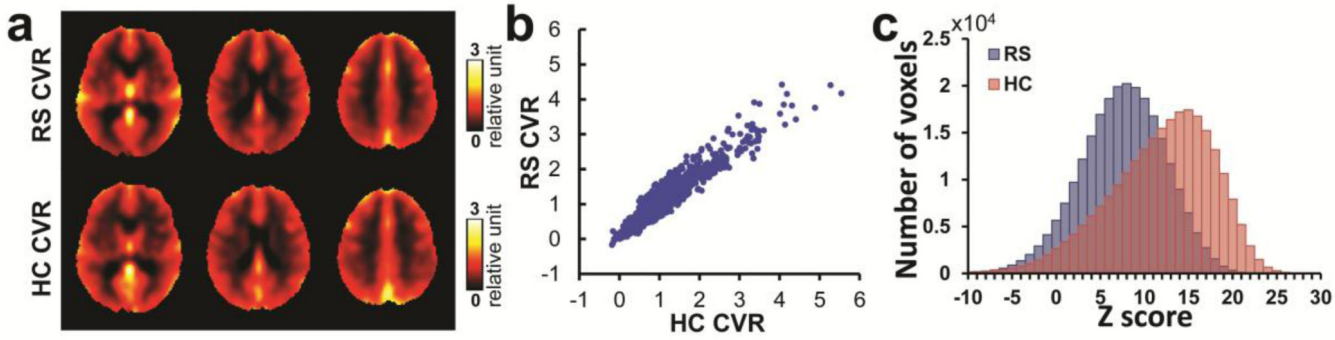

Figure 4.

Comparison between the group-averaged CVR obtained from resting-state scan (RS) and hypercapnia scan (HC) from 26 young healthy subjects. (a) The CVR maps obtained from the two scans. (b) Voxel-by-voxel scatter plot between the two maps (down-sampled by 5×5×5 voxels). (c) Average histograms of voxel-wise Z scores associated with CVR mapping using RS scan and HC scan, respectively.

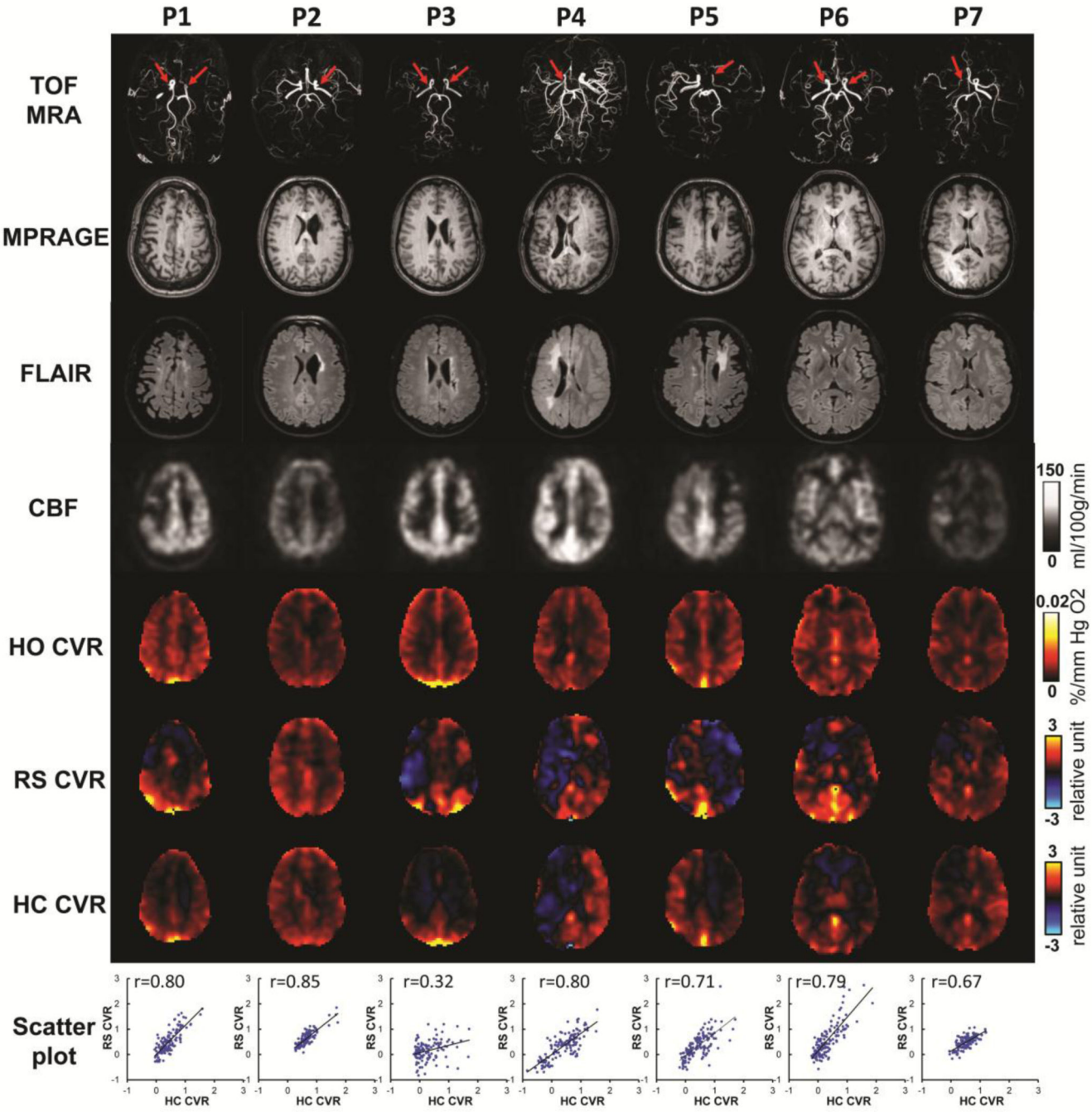

Figure 5.

Imaging results from the seven patients with Moyamoya diseases. Row 1: Time-of-flight (TOF) MR angiograms (MRA). Red arrows indicate the sties of arterial stenosis. Row 2: MPRAGE images. Row 3: T2-FLAIR images. Row 4: CBF maps. Row 5: venous CBV maps. Row 6: CVR maps using resting-state scan of these patients. Row 7: CVR maps from hypercapnia scan of these patients. Row 8: Scatter plots between the resting-state CVR map and hypercapnia CVR map for each patients.

Table 1

Demographic information of the patients with Moyamoya disease.

Subject	Age	Gender	Diagnosis	Treatment	Time since last treatment
P1	49	F	Bilateral supraclinoid occlusions	Bilateral bypass	19 months
P2	46	F	Left MCA occlusion	Left bypass	67 months
P3	30	F	Bilateral supraclinoid occlusions	Left bypass	3 months
P4	24	F	Right supraclinoid occlusion	Right bypass	4 months
P5	48	F	Left supraclinoid occlusion	Left bypass	40 months
P6	35	M	Bilateral MCA occlusions	Left bypass	6 months
P7	38	F	Right ICA occlusion	Right bypass	56 months